

LOFF Pairing vs. Breached Pairing in Asymmetric Fermion Superfluids

Lianyi He*, Meng Jin† and Pengfei Zhuang‡

Physics Department, Tsinghua University, Beijing 100084, China

A general analysis for the competition between breached pairing and LOFF pairing mechanisms in asymmetric fermion superfluids is presented in the frame of a four fermion interaction model in weak coupling region. For the superfluids with mismatched Fermi surfaces formed in different physical systems, we analytically and numerically calculated the coupled set of equations for the gap parameter, pair momentum, and thermodynamic potential. The breached pairing state is instable due to the Sarma instability or magnetic instability in any asymmetric system. While the LOFF state is stable only in a narrow asymmetry window in the case with fixed chemical potentials or fixed total number and chemical potential difference, it is stable in the whole coexistence region of breached pairing and LOFF pairing states in the case with fixed numbers of the two species. The LOFF state can even survive in the highly asymmetry region where the breached pairing state disappears.

PACS numbers: 13.60.Rj, 11.10.Wx, 25.75.-q

I. INTRODUCTION

The fermion pairing between different species with mismatched Fermi surfaces, which was discussed many years ago, promoted new interest in both theoretic and experimental studies in recent years. The mismatched Fermi surfaces can be realized, for instance, in a superconductor in an external magnetic field[1] or a strong spin-exchange field[2, 3, 4], an electronic gas with two species of electrons from different bands[5], a superconductor with overlapping bands[6, 7], trapped ions with dipolar interactions[8], a mixture of two types of fermionic cold atoms with different densities and/or masses[5, 9], an isospin asymmetric nuclear matter with proton-neutron pairing[10], and a neutral dense quark matter[11, 12, 13, 14, 15, 16, 17, 18, 19, 20, 21, 22]. In the early studies of superconductivity, Sarma[1] found a spatially uniform state where there exist gapless modes, namely it needs no energy for excitation of these quasi-particle modes. However, this state is energetically instable, compared with the fully gapped BCS state. This is called Sarma instability[1]. Recently, this instability was widely discussed in general case[23, 24] and in neutral color superconductivity[17, 18]. It is now accepted that the Sarma instability can be avoided through two possible ways, requiring unequal numbers of the two kinds of fermions[17, 18, 23] or a proper momentum structure of the attractive interaction between the two species[23]. The Sarma state is now also called breached pairing (BP) state, since in this state the dispersion relation of one branch of the quasi-particles has two zero points at momenta p_1 and p_2 where gapless excitations happen, and the superfluid Fermi liquid state in the regions $p < p_1$ and $p > p_2$ is breached by a normal Fermi liquid state in

the region $p_1 < p < p_2$.

The LOFF state which is a spatially non-uniform ground state with crystalline structure of order parameter was proposed in the study of superconductors in a strong spin-exchange field by Larkin, Ovchinnikov, Fulde and Ferrell[2, 3]. In this ground state, the translational and rotational symmetries of the system are spontaneously broken. In the study of asymmetric nuclear matter, asymmetric atomic fermion gas and color superconductivity, the LOFF phase has been widely investigated [25, 26, 27, 28, 29, 30, 31, 32, 33, 34, 35, 36, 37, 38, 39, 40].

While the Sarma instability can be avoided, a new instability of the BP state which is called magnetic instability in the literatures arises in the study of dense quark matter. It is found that the response to external color magnetic field in neutral dense quark matter in the BP state is paramagnetic, i.e., the Meissner mass squared of some gluons becomes negative[41, 42, 43, 44, 45]. In fact, the paramagnetic Meissner effect (PME) has been widely discussed in condensed matter physics[46, 47, 48, 49, 50, 51, 52, 53, 54, 55]. A general analysis for asymmetric superconductors shows that the PME is related to the breached pairing mechanism only, its existence is independent of the details of the attractive interactions[56]. It is recently pointed out that, in some systems the free energy of the LOFF state or some other exotic states is probably lower than that of the BP state[56, 57, 58, 59, 60, 61, 62, 63, 64]. However, this conclusion is obtained from the study in asymmetric systems with fixed chemical potentials. In many physical cases we are interested in, the chemical potentials are not directly fixed, instead the particle numbers are fixed or some other constraints on the numbers are required. For these systems, the magnetic instability is still not clear. In this paper we will give a general and systematic comparison between the BP and LOFF states in asymmetric fermion superfluids under different conditions which can lead to mismatched Fermi surfaces.

To be specific, we consider the model Hamiltonian with

*Email address: hely04@mails.tsinghua.edu.cn

†Email address: jin-m@mail.tsinghua.edu.cn

‡Email address: zhuangpf@mail.tsinghua.edu.cn

two species of fermions interacting with each other via a point interaction,

$$\hat{\mathcal{H}} = \int \frac{d^3\vec{p}}{(2\pi)^3} \left(\epsilon_p^a \hat{a}_{\vec{p}}^\dagger \hat{a}_{\vec{p}} + \epsilon_p^b \hat{b}_{\vec{p}}^\dagger \hat{b}_{\vec{p}} \right) - g \int \frac{d^3\vec{p} d^3\vec{p}' d^3\vec{k}}{(2\pi)^9} \hat{a}_{\vec{k}+\vec{p}}^\dagger \hat{b}_{\vec{k}-\vec{p}}^\dagger \hat{b}_{\vec{k}-\vec{p}'} \hat{a}_{\vec{k}+\vec{p}'}, \quad (1)$$

where $\hat{a}, \hat{b}, \hat{a}^\dagger$ and \hat{b}^\dagger are the annihilation and creation operators for the two species a and b , the coupling constant g is positive to keep the interaction attractive, and $\epsilon_p^a = \frac{p^2}{2m_a} - \mu_a$ and $\epsilon_p^b = \frac{p^2}{2m_b} - \mu_b$ are dispersion relations for the two species with masses m_a and m_b and chemical potentials μ_a and μ_b . We will consider in this paper only the case without mass difference between the two species, $m_a = m_b = m$, which is relevant for the study of cold atomic fermion gas, isospin asymmetric nuclear matter, and two flavor color superconducting quark matter.

Since the Hamiltonian (1) is non-renormalizable, it is necessary to introduce a regulator Λ which serves as a length scale in the problem. To make our study with the four-point interaction more general and suitable for different physical systems, we will fix the cutoff Λ by a comparison with a cutoff independent calculation in weak interaction limit. We focus on three types of asymmetric superfluids with mismatched Fermi surfaces induced by 1) fixed chemical potentials μ_a and μ_b , 2) fixed total particle number $n = n_a + n_b$ and chemical potential difference $\delta\mu = (\mu_b - \mu_a)/2$, and 3) fixed particle numbers n_a and n_b .

The paper is organized as follows. In Section II and III, we briefly review the formulism for the BP and LOFF states, respectively. In section IV, we analytically discuss the BP instabilities by considering gap fluctuations and pair momentum fluctuations, and show why the LOFF state may be more favored than the BP state. With the fixed cutoff and scaling formulism given in Section V, the numerical studies via directly calculating the thermodynamic potentials or free energies are presented in Sections VI, VII, and VIII for the above mentioned three kinds of asymmetric superfluids. We summarize in Section IX. We use the natural unit of $c = \hbar = 1$ through the paper.

II. BREACHED PAIRING SUPERFLUIDITY

The uniform ground state corresponds to the case where the two fermions of a Cooper pair have equal but opposite momenta. The Hamiltonian (1) can be reduced to

$$\hat{\mathcal{H}} = \int \frac{d^3\vec{p}}{(2\pi)^3} \left(\epsilon_p^a \hat{a}_{\vec{p}}^\dagger \hat{a}_{\vec{p}} + \epsilon_p^b \hat{b}_{\vec{p}}^\dagger \hat{b}_{\vec{p}} \right) - g \int \frac{d^3\vec{p}}{(2\pi)^3} \int \frac{d^3\vec{p}'}{(2\pi)^3} \hat{a}_{\vec{p}}^\dagger \hat{b}_{-\vec{p}}^\dagger \hat{b}_{-\vec{p}'} \hat{a}_{\vec{p}'}. \quad (2)$$

In mean field approximation, it can be further simplified as

$$\hat{\mathcal{H}} = \frac{\Delta^2}{g} + \int \frac{d^3\vec{p}}{(2\pi)^3} \left(\epsilon_p^a \hat{a}_{\vec{p}}^\dagger \hat{a}_{\vec{p}} + \epsilon_p^b \hat{b}_{\vec{p}}^\dagger \hat{b}_{\vec{p}} - \Delta \hat{a}_{\vec{p}}^\dagger \hat{b}_{-\vec{p}}^\dagger - \Delta \hat{b}_{-\vec{p}} \hat{a}_{\vec{p}} \right), \quad (3)$$

where we have defined the order parameter

$$\Delta = g \int \frac{d^3\vec{p}}{(2\pi)^3} \langle \hat{a}_{\vec{p}}^\dagger \hat{b}_{-\vec{p}}^\dagger \rangle \quad (4)$$

and choose it to be real. After a Bogliubov transformation $\hat{\alpha}_{\vec{p}} = \sin \theta \hat{a}_{\vec{p}} + \cos \theta \hat{b}_{-\vec{p}}^\dagger$, $\hat{\beta}_{\vec{p}} = \cos \theta \hat{b}_{-\vec{p}}^\dagger - \sin \theta \hat{a}_{\vec{p}}$ with the definitions $\cos 2\theta = \epsilon_S / \epsilon_\Delta$, $\sin 2\theta = -\Delta / \epsilon_\Delta$, and

$$\begin{aligned} \epsilon_S &= (\epsilon_p^a + \epsilon_p^b)/2, & \epsilon_A &= (\epsilon_p^a - \epsilon_p^b)/2, \\ \epsilon_\Delta &= \sqrt{\epsilon_S^2 + \Delta^2}, \end{aligned} \quad (5)$$

we derive the diagonal Hamiltonian in terms of the quasiparticles,

$$\hat{\mathcal{H}} = \frac{\Delta^2}{g} + \int \frac{d^3\vec{p}}{(2\pi)^3} \left(\epsilon_p^\alpha \hat{\alpha}_{\vec{p}}^\dagger \hat{\alpha}_{\vec{p}} + \epsilon_p^\beta \hat{\beta}_{\vec{p}}^\dagger \hat{\beta}_{\vec{p}} + \epsilon_p^b \right) \quad (6)$$

with the quasiparticle energies

$$\epsilon_p^\alpha = \epsilon_A + \epsilon_\Delta, \quad \epsilon_p^\beta = \epsilon_A - \epsilon_\Delta. \quad (7)$$

The key quantity to describe the thermal properties of a system is the thermodynamical potential. In mean field approximation, it is a summation of the contributions from the mean field and the two kinds of quasiparticles,

$$\begin{aligned} \Omega(\Delta) &= \frac{\Delta^2}{g} - \int \frac{d^3\vec{p}}{(2\pi)^3} \left[\left(\frac{\epsilon_p^\alpha}{2} + T \ln(1 + e^{-\frac{\epsilon_p^\alpha}{T}}) \right) \right. \\ &\quad \left. + \left(\frac{\epsilon_p^\beta}{2} + T \ln(1 + e^{-\frac{\epsilon_p^\beta}{T}}) \right) - \epsilon_S \right]. \end{aligned} \quad (8)$$

With the inverse fermion propagator matrix defined in the Nambu-Gorkov space,

$$\mathcal{G}^{-1}(i\omega_n, \vec{p}) = \begin{pmatrix} i\omega_n - \epsilon_p^a & \Delta \\ \Delta & i\omega_n + \epsilon_p^b \end{pmatrix}, \quad (9)$$

the thermodynamic potential can be expressed as

$$\Omega = \frac{\Delta^2}{g} - T \sum_n \int \frac{d^3\vec{p}}{(2\pi)^3} \text{Tr} \ln \mathcal{G}^{-1}(i\omega_n, \vec{p}) \quad (10)$$

in the imaginary time formulism of finite temperature field theory, where the summation is over the fermion frequency $\omega_n = (2n + 1)\pi T$. The explicit form of the fermion propagator can be easily evaluated as

$$\mathcal{G}(i\omega_n, \vec{p}) = \begin{pmatrix} \mathcal{G}_{11}(i\omega_n, \vec{p}) & \mathcal{G}_{12}(i\omega_n, \vec{p}) \\ \mathcal{G}_{21}(i\omega_n, \vec{p}) & \mathcal{G}_{22}(i\omega_n, \vec{p}) \end{pmatrix} \quad (11)$$

with the elements

$$\begin{aligned}\mathcal{G}_{11}(i\omega_n, \vec{p}) &= \frac{i\omega_n - \epsilon_A + \epsilon_S}{(i\omega_n - \epsilon_A)^2 - \epsilon_\Delta^2}, \\ \mathcal{G}_{22}(i\omega_n, \vec{p}) &= \frac{i\omega_n - \epsilon_A - \epsilon_S}{(i\omega_n - \epsilon_A)^2 - \epsilon_\Delta^2}, \\ \mathcal{G}_{12}(i\omega_n, \vec{p}) &= \frac{-\Delta}{(i\omega_n - \epsilon_A)^2 - \epsilon_\Delta^2}, \\ \mathcal{G}_{21}(i\omega_n, \vec{p}) &= \frac{-\Delta}{(i\omega_n - \epsilon_A)^2 - \epsilon_\Delta^2}.\end{aligned}\quad (12)$$

The gap parameter Δ as a function of temperature and chemical potentials is self-consistently determined through the gap equation,

$$\Delta = gT \sum_n \frac{d^3 \vec{p}}{(2\pi)^3} \mathcal{G}_{12}(i\omega_n, \vec{p}), \quad (13)$$

which is equivalent to the stationary condition of the thermodynamic potential, $\partial\Omega/\partial\Delta = 0$. Completing the frequency summation, the gap equation reads

$$\Delta(1 - gI_\Delta) = 0 \quad (14)$$

with the function I_Δ defined as

$$I_\Delta = \frac{1}{2} \int \frac{d^3 \vec{p}}{(2\pi)^3} \frac{f(\epsilon_p^\beta) - f(\epsilon_p^\alpha)}{\epsilon_\Delta}, \quad (15)$$

where $f(x) = 1/(e^{x/T} + 1)$ is the Fermi-Dirac distribution function.

The excitation spectra ϵ_p^α and ϵ_p^β can be read from the pole of the propagator. Without losing generality we choose $\epsilon_A > 0$ in the following. While one branch ϵ_p^α is fully gapped, the other one ϵ_p^β can cross the momentum axis and becomes gapless at two points p_1 and p_2 determined by the equation $\epsilon_p^\beta = 0$ and satisfying the constraint $p_F^a < p_1 < p_2 < p_F^b$, where p_F^a and p_F^b are the Fermi momenta of the species a and b at $T = 0$.

The gapless excitation of quasiparticles is directly related to the breached pairing phenomena. In terms of the quark propagator, the occupation numbers in momentum space can be expressed as

$$\begin{aligned}n_a(\vec{p}) &= T \lim_{\eta \rightarrow 0} \sum_n \mathcal{G}_{11}(i\omega_n, \vec{p}) e^{i\omega_n \eta}, \\ n_b(\vec{p}) &= -T \lim_{\eta \rightarrow 0} \sum_n \mathcal{G}_{22}(i\omega_n, \vec{p}) e^{-i\omega_n \eta}.\end{aligned}\quad (16)$$

Completing the Matsubara frequency summation, we have

$$\begin{aligned}n_a(\vec{p}) &= u_p^2 f(\epsilon_p^\alpha) + v_p^2 f(\epsilon_p^\beta), \\ n_b(\vec{p}) &= u_p^2 f(-\epsilon_p^\beta) + v_p^2 f(-\epsilon_p^\alpha) \\ &= 1 - u_p^2 f(\epsilon_p^\alpha) - v_p^2 f(\epsilon_p^\beta)\end{aligned}\quad (17)$$

with the definitions $u_p^2 = (1 + \epsilon_S/\epsilon_\Delta)/2$ and $v_p^2 = (1 - \epsilon_S/\epsilon_\Delta)/2$. At zero temperature, they are reduced

to

$$\begin{aligned}n_a(\vec{p}) &= v_p^2 \theta(\epsilon_\Delta - \epsilon_A) + u_p^2 \theta(-\epsilon_\Delta - \epsilon_A), \\ n_b(\vec{p}) &= v_p^2 \theta(\epsilon_\Delta + \epsilon_A) + u_p^2 \theta(-\epsilon_\Delta + \epsilon_A).\end{aligned}\quad (18)$$

For convenience, we define the average of the chemical potentials μ_a and μ_b and their difference,

$$\mu = (\mu_a + \mu_b)/2, \quad \delta\mu = (\mu_b - \mu_a)/2, \quad (19)$$

and then rewrite the dispersion relations of the quasiparticle excitations as

$$\begin{aligned}\epsilon_p^\alpha &= \delta\mu + \sqrt{(p^2/2m - \mu)^2 + \Delta^2}, \\ \epsilon_p^\beta &= \delta\mu - \sqrt{(p^2/2m - \mu)^2 + \Delta^2}.\end{aligned}\quad (20)$$

Without losing generality, we set $\delta\mu > 0$ which means $n_b \geq n_a$, where n_a and n_b are numbers of the species a and b ,

$$n_a = \int \frac{d^3 \vec{p}}{(2\pi)^3} n_a(\vec{p}), \quad n_b = \int \frac{d^3 \vec{p}}{(2\pi)^3} n_b(\vec{p}). \quad (21)$$

It is easy to see from the equation $\epsilon_p^\beta = 0$ that only in the case with $\Delta < \delta\mu$, there are gapless excitations at momenta

$$\begin{aligned}p_1 &= \sqrt{2m(\mu - \sqrt{\delta\mu^2 - \Delta^2})}, \\ p_2 &= \sqrt{2m(\mu + \sqrt{\delta\mu^2 - \Delta^2})}.\end{aligned}\quad (22)$$

In the gapless state, we have $n_a(\vec{p}) = n_b(\vec{p}) = v_p^2$ for $p < p_1$ and $p > p_2$ and $n_a(\vec{p}) = 0, n_b(\vec{p}) = 1$ for $p_1 < p < p_2$. Therefore, the superfluidity state with fermion pairing in the regions $p < p_1$ and $p > p_2$ is breached by the normal fermion gas in the region $p_1 < p < p_2$. This is the reason why people call the gapless state as breached pairing state. In the case with $\Delta > \delta\mu$, there is no gapless excitation, and the system is in BCS phase with $n_a(\vec{p}) = n_b(\vec{p}) = v_p^2$ for all p . The occupation numbers in breached pairing state are schematically illustrated in Fig.1.

III. LOFF PAIRING SUPERFLUIDITY

In the LOFF state, the Cooper pair possesses a total nonzero momentum $2\vec{q}$. In mean field approximation, the Hamiltonian

$$\begin{aligned}\hat{\mathcal{H}} &= \int \frac{d^3 \vec{p}}{(2\pi)^3} \left(\epsilon_p^a \hat{a}_p^\dagger \hat{a}_{\vec{p}} + \epsilon_p^b \hat{b}_p^\dagger \hat{b}_{\vec{p}} \right) \\ &\quad - g \int \frac{d^3 \vec{p}}{(2\pi)^3} \int \frac{d^3 \vec{p}'}{(2\pi)^3} \hat{a}_{\vec{q}+\vec{p}}^\dagger \hat{b}_{\vec{q}-\vec{p}}^\dagger \hat{b}_{\vec{q}-\vec{p}'} \hat{a}_{\vec{q}+\vec{p}'}\end{aligned}\quad (23)$$

is reduced to

$$\begin{aligned}\hat{\mathcal{H}} &= \frac{\Delta^2}{g} + \int \frac{d^3 \vec{p}}{(2\pi)^3} \left(\epsilon_{\vec{p}+\vec{q}}^a \hat{a}_{\vec{q}+\vec{p}}^\dagger \hat{a}_{\vec{q}+\vec{p}} \right. \\ &\quad \left. + \epsilon_{\vec{p}-\vec{q}}^b \hat{b}_{\vec{q}-\vec{p}}^\dagger \hat{b}_{\vec{q}-\vec{p}} - \Delta \hat{a}_{\vec{q}+\vec{p}}^\dagger \hat{b}_{\vec{q}-\vec{p}}^\dagger - \Delta \hat{b}_{\vec{q}-\vec{p}} \hat{a}_{\vec{q}+\vec{p}} \right)\end{aligned}\quad (24)$$

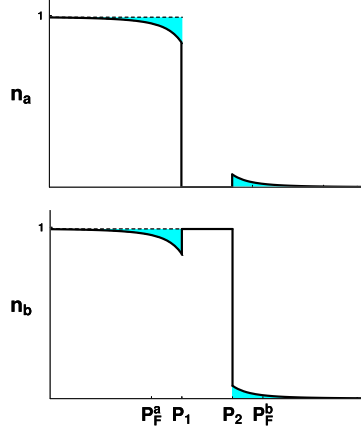


FIG. 1: The occupation numbers n_a and n_b as functions of momentum. p_F^a and p_F^b are Fermi momenta of species a and b , and p_1 and p_2 are the two roots of the dispersion equation $\epsilon_p^\beta = 0$. The fermion pairing in the regions $p < p_1$ and $p > p_2$ is breached by the normal fermion liquid in the region $p_1 < p < p_2$.

with LOFF energies $\epsilon_{\vec{p}+\vec{q}}^a = \frac{(\vec{p}+\vec{q})^2}{2m_a} - \mu_a$ and $\epsilon_{\vec{p}-\vec{q}}^b = \frac{(\vec{p}-\vec{q})^2}{2m_b} - \mu_b$. Here we have defined the LOFF order parameter

$$\Delta = g \int \frac{d^3\mathbf{p}}{(2\pi)^3} \langle \hat{a}_{\vec{q}+\vec{p}}^\dagger \hat{b}_{\vec{q}-\vec{p}}^\dagger \rangle \quad (25)$$

and choose it to be real again. In coordinate space, this order parameter has a single plane wave crystalline structure $\langle \hat{\Psi}_a(\vec{x}) \hat{\Psi}_b(\vec{x}) \rangle = \Delta e^{2i\vec{q} \cdot \vec{x}}$. Taking a modified Bogliubov transformation $\hat{A}_{\vec{p},\vec{q}} = \cos \phi \hat{a}_{\vec{q}+\vec{p}} + \sin \phi \hat{b}_{\vec{q}-\vec{p}}^\dagger$, $\hat{B}_{\vec{p},\vec{q}} = \cos \phi \hat{b}_{\vec{q}-\vec{p}}^\dagger - \sin \phi \hat{a}_{\vec{q}+\vec{p}}$ with $\cos 2\phi = E_S/E_\Delta$, $\sin 2\phi = -\Delta/E_\Delta$, we obtain the diagonal Hamiltonian in terms of the quasiparticles,

$$\hat{H} = \frac{\Delta^2}{g} + \int \frac{d^3\vec{p}}{(2\pi)^3} \left(E_{\vec{p},\vec{q}}^A \hat{A}_{\vec{p},\vec{q}}^\dagger \hat{A}_{\vec{p},\vec{q}} + E_{\vec{p},\vec{q}}^B \hat{B}_{\vec{p},\vec{q}}^\dagger \hat{B}_{\vec{p},\vec{q}} + \epsilon_{\vec{p}-\vec{q}}^b \right), \quad (26)$$

where the quasiparticle energies are defined as

$$\begin{aligned} E_{\vec{p},\vec{q}}^A &= E_A + E_\Delta, & E_{\vec{p},\vec{q}}^B &= E_A - E_\Delta, \\ E_S &= \frac{\epsilon_{\vec{p}+\vec{q}}^a + \epsilon_{\vec{p}-\vec{q}}^b}{2}, & E_A &= \frac{\epsilon_{\vec{p}+\vec{q}}^a - \epsilon_{\vec{p}-\vec{q}}^b}{2}, \\ E_\Delta &= \sqrt{E_S^2 + \Delta^2}. \end{aligned} \quad (27)$$

With the quasiparticles, the thermodynamic potential in mean field approximation reads

$$\begin{aligned} \Omega(\Delta, \vec{q}) &= \frac{\Delta^2}{g} - \int \frac{d^3\vec{p}}{(2\pi)^3} \left[\left(\frac{E_{\vec{p},\vec{q}}^A}{2} + T \ln(1 + e^{-\frac{E_{\vec{p},\vec{q}}^A}{T}}) \right) \right. \\ &\quad \left. + \left(\frac{E_{\vec{p},\vec{q}}^B}{2} + T \ln(1 + e^{-\frac{E_{\vec{p},\vec{q}}^B}{T}}) \right) - E_S \right], \end{aligned} \quad (28)$$

which is now a function of the pair momentum \vec{q} .

Again, the thermodynamic potential can be expressed as

$$\Omega(\Delta, \vec{q}) = \frac{\Delta^2}{g} - T \sum_n \int \frac{d^3\vec{p}}{(2\pi)^3} \text{Tr} \ln \mathcal{S}^{-1}(i\omega_n, \vec{p}) \quad (29)$$

in terms of the inverse LOFF propagator

$$\mathcal{S}^{-1}(i\omega_n, \vec{p}) = \begin{pmatrix} i\omega_n - \epsilon_{\vec{p}+\vec{q}}^a & \Delta \\ \Delta & i\omega_n + \epsilon_{\vec{p}-\vec{q}}^b \end{pmatrix}. \quad (30)$$

The explicit form of the propagator can be written as

$$\mathcal{S}(i\omega_n, \vec{p}) = \begin{pmatrix} \mathcal{S}_{11}(i\omega_n, \vec{p}) & \mathcal{S}_{12}(i\omega_n, \vec{p}) \\ \mathcal{S}_{21}(i\omega_n, \vec{p}) & \mathcal{S}_{22}(i\omega_n, \vec{p}) \end{pmatrix} \quad (31)$$

with the elements

$$\begin{aligned} \mathcal{S}_{11}(i\omega_n, \vec{p}) &= \frac{i\omega_n - E_A + E_S}{(i\omega_n - E_A)^2 - E_\Delta^2}, \\ \mathcal{S}_{22}(i\omega_n, \vec{p}) &= \frac{i\omega_n - E_A - E_S}{(i\omega_n - E_A)^2 - E_\Delta^2}, \\ \mathcal{S}_{12}(i\omega_n, \vec{p}) &= \frac{-\Delta}{(i\omega_n - E_A)^2 - E_\Delta^2}, \\ \mathcal{S}_{21}(i\omega_n, \vec{p}) &= \frac{-\Delta}{(i\omega_n - E_A)^2 - E_\Delta^2}. \end{aligned} \quad (32)$$

The gap equation which determines the order parameter Δ self-consistently is again related to the off-diagonal element of the propagator matrix,

$$\Delta = gT \sum_n \frac{d^3\vec{p}}{(2\pi)^3} \mathcal{S}_{12}(i\omega_n, \vec{p}), \quad (33)$$

which is still equivalent to the stationary condition of the thermodynamic potential, $\partial\Omega/\partial\Delta = 0$. After the summation over the fermion frequency, it becomes

$$\Delta(1 - gI_\Delta) = 0, \quad (34)$$

the function I_Δ is now defined as

$$I_\Delta = \frac{1}{2} \int \frac{d^3\vec{p}}{(2\pi)^3} \frac{f(E_{\vec{p},\vec{q}}^B) - f(E_{\vec{p},\vec{q}}^A)}{E_\Delta}. \quad (35)$$

While the gap equations in BP state and LOFF state look the same, the gap parameter Δ in LOFF state depends on the pair momentum \vec{q} . In the following we choose a suitable frame where the z axis is along the direction of the pair momentum, $\vec{q} = (0, 0, q)$. The physical pair momentum q is determined by the minimal thermodynamic potential, $\partial\Omega/\partial q = 0$. Calculating the first order derivative of (28) with respect to q , the gap equation for q is explicitly written as

$$\begin{aligned} 0 &= \int \frac{d^3\vec{p}}{(2\pi)^3} \left[(1 - f(E_{\vec{p},\vec{q}}^A) - f(E_{\vec{p},\vec{q}}^B)) \frac{\partial E_A}{\partial q} \right. \\ &\quad \left. - \left(1 + (f(E_{\vec{p},\vec{q}}^A) - f(E_{\vec{p},\vec{q}}^B)) \frac{E_S}{E_\Delta} \right) \frac{\partial E_S}{\partial q} \right]. \end{aligned} \quad (36)$$

It is easy to see that $q = 0$ is a trivial solution of the equation, which corresponds to the uniform ground state.

Using the chemical potentials μ and $\delta\mu$ introduced in Section II, the dispersion relations of the elementary excitations can be written as

$$\begin{aligned} E_{\vec{p},\vec{q}}^A &= \delta\mu + \frac{pq}{m}x + \sqrt{\left(\frac{p^2 + q^2}{2m} - \mu\right)^2 + \Delta^2}, \\ E_{\vec{p},\vec{q}}^B &= \delta\mu + \frac{pq}{m}x - \sqrt{\left(\frac{p^2 + q^2}{2m} - \mu\right)^2 + \Delta^2} \end{aligned} \quad (37)$$

with the variable $x = \cos\theta$, where θ is the angle between the momenta \vec{p} and \vec{q} . In many of the previous investigations, the term $q^2/2m$ was neglected and the term pqx/m was approximated by $v_F qx$ [2, 3, 4] with the Fermi velocity v_F . In this paper we will not employ this approximation.

The occupation numbers are still determined through the diagonal elements of the fermion propagator,

$$\begin{aligned} n_a(\vec{p}) &= T \lim_{\eta \rightarrow 0} \sum_n \mathcal{S}_{11}(i\omega_n, \vec{p}) e^{i\omega_n \eta}, \\ n_b(\vec{p}) &= -T \lim_{\eta \rightarrow 0} \sum_n \mathcal{S}_{22}(i\omega_n, \vec{p}) e^{-i\omega_n \eta}. \end{aligned} \quad (38)$$

Completing the Matsubara frequency summation, we obtain

$$\begin{aligned} n_a(\vec{p}) &= U_p^2 f(E_{\vec{p},\vec{q}}^A) + V_p^2 f(E_{\vec{p},\vec{q}}^B), \\ n_b(\vec{p}) &= U_p^2 f(-E_{\vec{p},\vec{q}}^B) + V_p^2 f(-E_{\vec{p},\vec{q}}^A) \\ &= 1 - U_p^2 f(E_{\vec{p},\vec{q}}^B) - V_p^2 f(E_{\vec{p},\vec{q}}^A) \end{aligned} \quad (39)$$

with the definition $U_p^2 = (1 + E_S/E_\Delta)/2$ and $V_p^2 = (1 - E_S/E_\Delta)/2$. At zero temperature, they are reduced to

$$\begin{aligned} n_a(\vec{p}) &= V_p^2 \theta(E_\Delta - E_A) + U_p^2 \theta(-E_\Delta - E_A), \\ n_b(\vec{p}) &= V_p^2 \theta(E_\Delta + E_A) + U_p^2 \theta(-E_\Delta + E_A). \end{aligned} \quad (40)$$

In the LOFF state, the dispersion relations of quasi-particles as well as the occupation numbers become anisotropic, they depend on the angle variable x .

IV. PERTURBING THE BP STATE

In this section, we will discuss some possible instabilities of the breached pairing state. From the analytic analysis, we will see that there are two types of instabilities in the BP phase. One is the Sarma instability which was found many years ago, and the other is the magnetic instability which was recently found in the study of gapless superconductivity.

We first discuss the instability introduced by condensate fluctuations. Expanding the difference in the thermodynamic potential induced by an infinitely small condensate δ ,

$$\Omega(\Delta + \delta) - \Omega(\Delta) = \frac{\partial \Omega}{\partial \Delta} \delta + \frac{1}{2} \frac{\partial^2 \Omega}{\partial \Delta^2} \delta^2 + \dots, \quad (41)$$

and taking into account the fact that the above linear term vanishes due to the gap equation $\partial \Omega / \partial \Delta = 0$, and employing the derivative expansion for any two independent matrices A and B ,

$$\text{Tr} \ln(A^{-1} + B) = \text{Tr} \ln A^{-1} - \sum_{n=1}^{\infty} \frac{(-1)^n}{n} \text{Tr}(AB)^n, \quad (42)$$

the gap susceptibility defined by

$$\kappa_\Delta = \frac{\partial^2 \Omega}{\partial \Delta^2} \quad (43)$$

can be expressed as

$$\kappa_\Delta = \frac{1}{g} + T \sum_n \int \frac{d^3 \vec{p}}{(2\pi)^3} (\mathcal{G}_{11} \mathcal{G}_{22} + \mathcal{G}_{12} \mathcal{G}_{21}). \quad (44)$$

At zero temperature, it is evaluated as

$$\kappa_\Delta = \int_0^\infty \frac{dp p^2}{2\pi^2} u_p^2 v_p^2 \left[\frac{\theta(\epsilon_\Delta - \delta\mu)}{\epsilon_\Delta} - \delta(\epsilon_\Delta - \delta\mu) \right]. \quad (45)$$

For the BCS state which satisfies the constraint $\Delta > \delta\mu$, the δ -function disappears automatically, and κ_Δ is obviously positive which means that the state is stable. For the BP state with $\Delta < \delta\mu$, the integral over the δ -function becomes nonzero and dominates the susceptibility. In this case, we have $\kappa_\Delta < 0$ which indicates that the state is unstable. This is the so-called Sarma instability.

For the systems with fixed chemical potentials μ_a and μ_b or fixed total chemical potential μ and chemical potential difference $\delta\mu$, we can directly compare $\delta\mu$ with Δ and see if the state is stable. However, for the systems under some constraints on particle numbers, the grand canonical ensemble should be replaced by canonical ensemble, and the essential quantity to describe the thermodynamics of the systems is the free energy F instead of the thermodynamic potential Ω . In this case, the chemical potentials are no longer independent thermodynamic variables, Δ and $\delta\mu$ should be determined self-consistently via solving the coupled set of equations for the gap parameter and the constraints on the particle numbers. Therefore, it is not convenient to judge the instability of the BP state through κ_Δ . On the other hand, when the number difference between the two species is fixed, the BCS solution is ruled out, and only the BP state survives[17, 18]. A direct way for the instability analysis is to compare the thermodynamic potentials or free energies themselves in BP and LOFF states, and see which one is more stable.

We now turn to discuss another kind of BP instability induced by pair momentum fluctuations. We perturb the BP state with an infinitely small LOFF momentum q and calculate the momentum susceptibility

$$\kappa_q = \frac{\partial^2 \Omega}{\partial q^2}. \quad (46)$$

Expanding the thermodynamic potential (28) in the LOFF state around $q = 0$,

$$\Omega(\Delta, q) - \Omega(\Delta, 0) = \frac{\partial \Omega}{\partial q} \Big|_{q=0} q + \frac{1}{2} \frac{\partial^2 \Omega}{\partial q^2} \Big|_{q=0} q^2 + \dots, \quad (47)$$

and taking into account the gap equation for the pair momentum, $\partial \Omega / \partial q = 0$, and the derivative expansion (42), we can express the momentum susceptibility as

$$\kappa_q = \frac{n}{m} + \frac{T}{3} \sum_n \int \frac{d^3 \vec{p}}{(2\pi)^3} \frac{p^2}{m^2} (\mathcal{G}_{11} \mathcal{G}_{11} + \mathcal{G}_{22} \mathcal{G}_{22} + 2\mathcal{G}_{12} \mathcal{G}_{21}), \quad (48)$$

where $n = n_a + n_b$ is the total fermion density. At zero temperature, κ_q is reduced to

$$\kappa_q = \frac{n}{m} \left[1 - \eta \frac{\delta \mu \theta(\delta \mu - \Delta)}{\sqrt{\delta \mu^2 - \Delta^2}} \right] \quad (49)$$

with the coefficient $\eta = (p_1^3 + p_2^3) / (6\pi^2 n)$. Since the total fermion density n at $T = 0$ can be expressed as

$$n = \frac{p_1^3 + p_2^3}{6\pi^2} + \frac{1}{\pi^2} \left(- \int_0^{p_1} dp p^2 u_p^2 + \int_{p_2}^\infty dp p^2 v_p^2 \right), \quad (50)$$

and the two integrals in the bracket which are related to the upper and lower shadow regions of $n_a(\vec{p})$ and $n_b(\vec{p})$ in Fig.1 are very small and can be neglected[56], the coefficient η is approximately equal to 1 and κ_q can be expressed as

$$\kappa_q \approx \frac{n}{m} \left[1 - \frac{\delta \mu \theta(\delta \mu - \Delta)}{\sqrt{\delta \mu^2 - \Delta^2}} \right]. \quad (51)$$

From this result, it is easy to see that in the BP phase with $\Delta < \delta \mu$, κ_q becomes negative. This is the so called magnetic instability, since it is directly related to the negative Meissner mass squared, if the fermions are charged. As we mentioned above, however, under some constraints on particle numbers, it is not convenient to judge the magnetic instability by the comparison of Δ with $\delta \mu$. In this case, it is better to calculate directly the thermodynamic potentials or free energies in the BP and LOFF states.

V. SCALING SUPERFLUIDITY

There are two parameters in the four-point interaction (1), the coupling constant and the momentum cutoff. For a specific system, they can be fixed by fitting some measurable quantities. Since our purpose is a general comparison between the BP and LOFF states, we do not focus on the details of a specific system. To this end, we replace the coupling constant by a dimensionless

quantity and fix the cutoff from a comparison with the calculation in weak coupling limit.

In nonrelativistic fermion systems such as atomic fermion gas and nuclear matter, the four-fermion coupling g is related to the s -wave scattering length a_S at tree level,

$$g = -\frac{4\pi a_S}{m}. \quad (52)$$

For attractive interaction, there is always $a_S < 0$. In the following we take $a = |a_S|$.

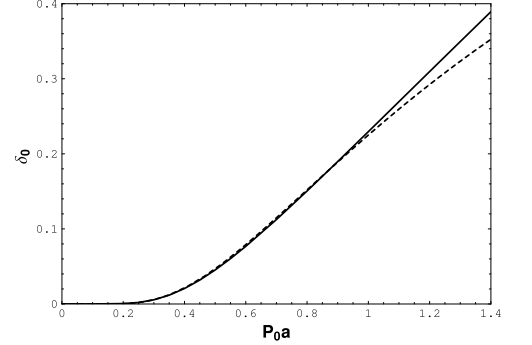


FIG. 2: The gap parameter, scaled by the Fermi energy μ_0 , as a function of the dimensionless coupling strength $p_0 a$ for a symmetric superfluid. The solid and dashed lines represent, respectively, the numerical solution of the gap equation (53) with a hard cutoff $\Lambda = \sqrt{2}$ and its analytic result (55) in weak coupling limit.

Denoting the chemical potential or Fermi energy in a symmetric superfluid as μ_0 and the corresponding Fermi momentum as $p_0 = \sqrt{2m\mu_0}$, and changing the integral variable from p to $z = (p/p_0)^2$, the gap equation to determine the nonzero condensate in the symmetric system at $T = 0$ can be expressed in terms of the dimensionless quantities $z, \delta_0 = \Delta_0/\mu_0$ and $p_0 a$ instead of p, Δ_0 and g ,

$$\int_0^\Lambda \frac{\sqrt{z} dz}{\sqrt{(z-1)^2 + \delta_0^2}} = \frac{\pi}{p_0 a}, \quad (53)$$

where Λ is the up limit of z . The above gap equation can be approximately solved with the analytic result in weak coupling limit

$$\delta_0 \simeq \frac{8\sqrt{\Lambda^2 - 1}}{e^2} e^{-\frac{\pi}{2p_0 a}}. \quad (54)$$

The cutoff Λ can be fixed by comparing the scaled gap parameter (54) with the result obtained from some cutoff independent gap equation. In the following, we choose $\Lambda = \sqrt{2}$ to fit the result in the weak interaction limit[65]

$$\delta_0 \simeq \frac{8}{e^2} e^{-\frac{\pi}{2p_0 a}}. \quad (55)$$

The comparison between the analytic result (54) and the numerical solution of the gap equation (53) with $\Lambda =$

$\sqrt{2}$ is shown in Fig.2. When the interaction strength is not very strong, $p_0 a < 1$, the cutoff does not make remarkable difference in the calculation of superfluidity. Therefore, our model with a hard cutoff is a good enough approximation in weak interaction region. In this paper we restrict ourselves in the region $p_0 a < 1$.

Now the characteristic of a specific asymmetric system is described in our treatment by the dimensionless parameter $p_0 a$. To have a general comparison between the BP and LOFF states, we scale all the quantities with energy dimension by the Fermi energy μ_0 and all the quantities with momentum dimension by the Fermi momentum p_0 ,

$$z = (p/p_0)^2, \quad z_q = (q/p_0)^2, \quad \nu_a = \mu_a/\mu_0, \quad \nu_b = \mu_b/\mu_0, \quad \nu = (\mu/\mu_0), \quad \delta\nu = \delta\mu/\mu_0, \quad \delta = \Delta/\mu_0, \quad t = T/\mu_0. \quad (56)$$

With these dimensionless quantities, we obtain the scaled gap equations

$$\delta \left[\int_0^\Lambda dz \sqrt{z} \frac{f(\epsilon_z^\beta) - f(\epsilon_z^\alpha)}{\sqrt{(z - \nu)^2 + \delta^2}} - \frac{\pi}{p_0 a} \right] = 0 \quad (57)$$

for the uniform gap parameter δ , and

$$\begin{aligned} \delta \left[\int_0^\Lambda dz \sqrt{z} \int_{-1}^1 dx \frac{f(E_{z,x}^B) - f(E_{z,x}^A)}{\sqrt{(z + z_q - \nu)^2 + \delta^2}} - \frac{2\pi}{p_0 a} \right] &= 0, \\ \int_0^\Lambda dz \sqrt{z} \int_{-1}^1 dx \left[x \sqrt{\frac{z}{z_q}} (f(E_{z,x}^A) + f(E_{z,x}^B)) + \frac{z + z_q - \nu}{\sqrt{(z + z_q - \nu)^2 + \delta^2}} (f(E_{z,x}^A) - f(E_{z,x}^B)) + 1 \right] &= 0 \end{aligned} \quad (58)$$

for the LOFF gap parameter δ and the LOFF pair momentum z_q , the scaled thermodynamic potentials

$$\frac{\Omega}{E_0} = \frac{\pi\delta^2}{2p_0 a} - \int_0^\Lambda dz \sqrt{z} \left[\left(\frac{\epsilon_z^\alpha}{2} + t \ln(1 + e^{-\frac{\epsilon_z^\alpha}{t}}) \right) + \left(\frac{\epsilon_z^\beta}{2} + t \ln(1 + e^{-\frac{\epsilon_z^\beta}{t}}) \right) - (z - \nu) \right] \quad (59)$$

for the uniform state, and

$$\frac{\Omega}{E_0} = \frac{\pi\delta^2}{2p_0 a} - \frac{1}{2} \int_0^\Lambda dz \sqrt{z} \int_{-1}^1 dx \left[\left(\frac{E_{z,x}^A}{2} + t \ln(1 + e^{-\frac{E_{z,x}^A}{t}}) \right) + \left(\frac{E_{z,x}^B}{2} + t \ln(1 + e^{-\frac{E_{z,x}^B}{t}}) \right) - (z + z_q - \nu) \right] \quad (60)$$

for the LOFF state, and the scaled number densities

$$\begin{aligned} \frac{n_a}{n_0} &= \int_0^\Lambda dz \sqrt{z} [u_z^2 f(\epsilon_z^\alpha) + v_z^2 f(\epsilon_z^\beta)], \\ \frac{n_b}{n_0} &= \int_0^\Lambda dz \sqrt{z} [1 - u_z^2 f(\epsilon_z^\beta) - v_z^2 f(\epsilon_z^\alpha)] \end{aligned} \quad (61)$$

for the uniform state, and

$$\begin{aligned} \frac{n_a}{n_0} &= \frac{1}{2} \int_0^\Lambda dz \sqrt{z} \int_{-1}^1 dx [U_z^2 f(E_{z,x}^A) + V_z^2 f(E_{z,x}^B)], \\ \frac{n_b}{n_0} &= \frac{1}{2} \int_0^\Lambda dz \sqrt{z} \int_{-1}^1 dx [1 - U_z^2 f(E_{z,x}^B) - V_z^2 f(E_{z,x}^A)] \end{aligned} \quad (62)$$

for the LOFF state. Here the normalization constants n_0 and E_0 are chosen to be $n_0 = p_0^3/(4\pi^2)$ and $E_0 = p_0^5/(8\pi^2 m)$, the quasiparticle energies and the functions u, v, U, V defined in Sections II and III are reexpressed in

terms of the dimensionless quantities,

$$\begin{aligned} \epsilon_z^\alpha &= \delta\nu + \sqrt{(z - \nu)^2 + \delta^2}, \\ \epsilon_z^\beta &= \delta\nu - \sqrt{(z - \nu)^2 + \delta^2}, \\ E_{z,x}^A &= \delta\nu + 2x\sqrt{zz_q} + \sqrt{(z + z_q - \nu)^2 + \delta^2}, \\ E_{z,x}^B &= \delta\nu + 2x\sqrt{zz_q} - \sqrt{(z + z_q - \nu)^2 + \delta^2}, \\ u_z^2 &= \frac{1}{2} \left(1 + (z - \nu)/\sqrt{(z - \nu)^2 + \delta^2} \right), \\ v_z^2 &= \frac{1}{2} \left(1 - (z - \nu)/\sqrt{(z - \nu)^2 + \delta^2} \right), \\ U_z^2 &= \frac{1}{2} \left(1 + (z + z_q - \nu)/\sqrt{(z + z_q - \nu)^2 + \delta^2} \right), \\ V_z^2 &= \frac{1}{2} \left(1 - (z + z_q - \nu)/\sqrt{(z + z_q - \nu)^2 + \delta^2} \right), \end{aligned} \quad (63)$$

and f is now defined as $f(x) = 1/(e^{x/t} + 1)$.

VI. FIXED CHEMICAL POTENTIALS

We now start the numerical calculations of the thermodynamic potentials (59,60) together with the gap equations (57,58) to find the stable state among the normal, BCS, BP and LOFF states. The four states are defined through the solutions of the gap equations as

- (1) normal phase with $\Delta = 0$,
- (2) BCS phase with $\Delta \neq 0, q = 0$ and $\Delta > \delta\mu$,
- (3) BP phase with $\Delta \neq 0, q = 0$ and $\Delta < \delta\mu$,
- (4) LOFF phase with $\Delta \neq 0, q \neq 0$.

In this section we consider the case of fixed chemical potentials μ_a and μ_b with $\mu_a \neq \mu_b$. In this case, the system is connected to reservoirs of each species and the particle numbers are not conserved. To be specific, we take $\mu = \mu_0$, namely $\nu = 1$ in the calculations. Fig.3 shows the condensate Δ , scaled by its value Δ_0 in the symmetric system defined in (53), as a function of the chemical potential difference $\delta\mu$, also scaled by Δ_0 , at $p_0a = 0.4$ and $T = 0$. We compare first the three uniform phases. The normal solution with $\Delta = 0$ is always a trivial solution of the gap equations which describes the normal phase without superfluidity, the BCS solution does not change with increasing $\delta\mu$ and keeps its symmetric value until $\delta\mu = \Delta_0$, and the BP solution starts to appear at $\delta\mu = \Delta_0/2$ and satisfies $\Delta < \delta\mu$ in the region $\Delta_0/2 < \delta\mu < \Delta_0$. From the analytic analysis in Section IV, the BP state is unstable. This can be seen clearly from the thermodynamics as a function of the scaled condensate Δ/Δ_0 for three values of scaled chemical potential difference $\delta\mu/\Delta_0$, shown in Fig.4. For $\delta\mu < \Delta_0/2$, there are a maximum at $\Delta = 0$ and a minimum at $\Delta = \Delta_0$, corresponding, respectively, to the normal phase and BCS phase, and for $\Delta_0/2 < \delta\mu < \Delta_0/\sqrt{2}$, there are a maximum at $0 < \Delta < \Delta_0$, a minimum at $\Delta = 0$ and the lowest minimum at $\Delta = \Delta_0$, corresponding, respectively, to the BP state, normal state and BCS state. For $\delta\mu > \Delta_0/\sqrt{2}$, the maximum is still located at $0 < \Delta < \Delta_0$, but the local minimum and the lowest minimum exchange positions. Therefore, among the three uniform phases the BCS phase is stable in the region $0 < \delta\mu < \Delta_0/\sqrt{2}$ and the normal phase becomes stable for $\delta\mu > \Delta_0/\sqrt{2}$.

We now include the spatially non-uniform state. The scaled LOFF gap Δ/Δ_0 and LOFF momentum q/p_0 are shown in Figs.3 and 5 as functions of the scaled chemical potential difference $\delta\mu/\Delta_0$ at $p_0a = 0.4$ and $T = 0$. The LOFF state starts at $\delta\mu = 0.635\Delta_0$ and there are two branches which we call LOFF1 and LOFF2. To find the true ground state, we compared the thermodynamic potentials as functions of $\delta\mu/\Delta_0$ for the four phases in Fig.6. It is easy to see that, below $\delta\mu_1 \simeq \Delta_0/\sqrt{2} = 0.707\Delta_0$ the LOFF1 and LOFF2 are unstable and the system is in BCS state, above $\delta\mu_2 \simeq 0.754\Delta_0$ the normal liquid state becomes stable, and in between $\delta\mu_1$ and $\delta\mu_2$ the LOFF2 state is the true ground state. The critical values $\delta\mu_1$ and $\delta\mu_2$ for the LOFF state agree with the an-

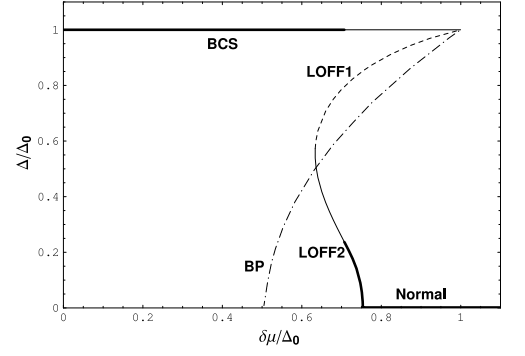


FIG. 3: The scaled gap parameter Δ/Δ_0 as a function of the scaled chemical potential difference $\delta\mu/\Delta_0$ at $p_0a = 0.4$ and $T = 0$ for normal, BCS, BP and LOFF (including LOFF1 by dashed line and LOFF2 by solid line) states. The thick lines indicate the real ground states in different regions.

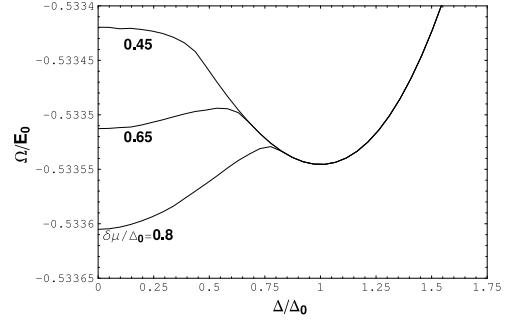


FIG. 4: The scaled thermodynamic potential as a function of the scaled gap parameter at $p_0a = 0.4, T = 0$ and $q = 0$ for three chemical potential regions, $0 < \delta\mu/\Delta_0 < 1/2$, $1/2 < \delta\mu/\Delta_0 < 1/\sqrt{2}$ and $\delta\mu/\Delta_0 > 1/\sqrt{2}$.

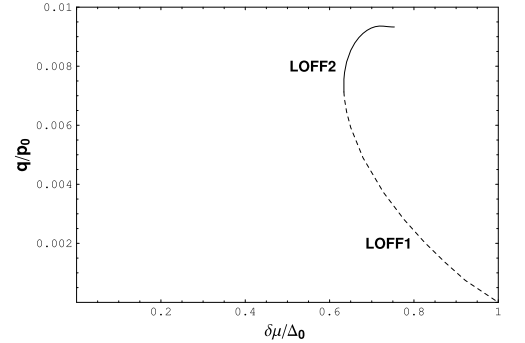


FIG. 5: The scaled LOFF momentum as a function of the scaled chemical potential difference at $p_0a = 0.4$ and $T = 0$ for LOFF1 and LOFF2.

alytical result obtained in weak coupling limit[65]. In Fig.7 we showed $\delta\mu_1/\Delta_0$ and $\delta\mu_2/\Delta_0$ as functions of p_0a . In small coupling region, they are almost constants and agree well with the analytical result, while when the cou-

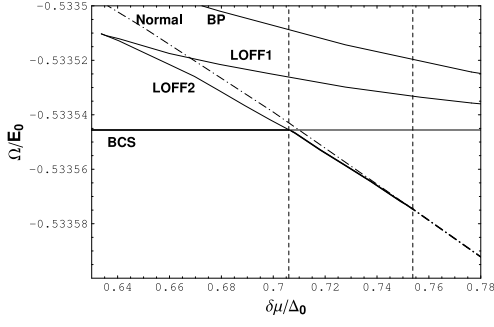


FIG. 6: The scaled thermodynamic potential as a function of the scaled chemical potential difference at $p_0a = 0.4$ and $T = 0$ for normal, BCS, BP, LOFF1, and LOFF2 states. The thick lines indicate the real ground states in different regions.

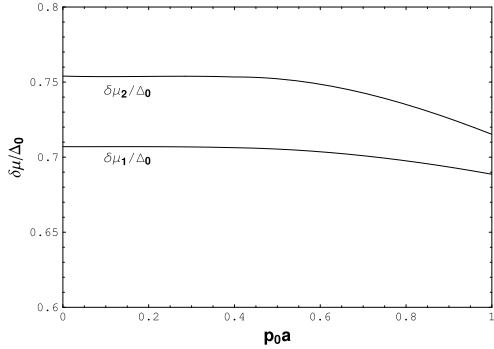


FIG. 7: The starting and ending chemical potential difference $\delta\mu_1$ and $\delta\mu_2$ for the LOFF state as functions of p_0a .

pling is strong enough, the LOFF window becomes small. Our numerical results are qualitatively consistent with the previous investigations[2, 3, 4].

VII. FIXED TOTAL DENSITY AND CHEMICAL POTENTIAL DIFFERENCE

We consider in this section the case of fixed total particle number density $n = n_a + n_b$ and chemical potential difference $\delta\mu = (\mu_b - \mu_a)/2$. In this case, the total particle number is conserved but the number exchange between the two species is still possible. Because of the number constraint, we should use the free energy

$$F = \Omega + \mu n \quad (64)$$

as essential quantity to describe the thermodynamics of the system. The thermodynamic variables are now n (instead of μ) and $\delta\mu$.

We still compare first the three uniform states by calculating the coupled set of equations for the thermodynamic potential (59), the gap equation (57) and the total

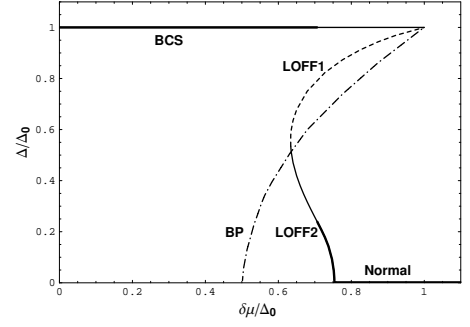


FIG. 8: The scaled gap parameter Δ/Δ_0 as a function of the scaled chemical potential difference $\delta\mu/\Delta_0$ at $p_0a = 0.4$ and $T = 0$ for normal, BCS, BP, LOFF1, and LOFF2 states. The thick lines indicate the real ground state in different regions.

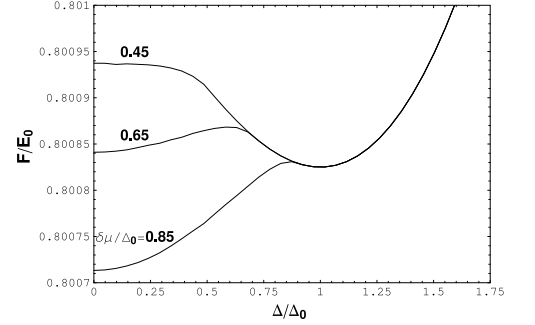


FIG. 9: The scaled free energy as a function of the scaled gap parameter at $p_0a = 0.4$, $T = 0$ and $q = 0$ for three chemical potential regions, $0 < \delta\mu/\Delta_0 < 1/2$, $1/2 < \delta\mu/\Delta_0 < 1/\sqrt{2}$ and $\delta\mu/\Delta_0 > 1/\sqrt{2}$.

particle number

$$\int_0^\Lambda dz \sqrt{z} [1 + (u_z^2 - v_z^2) (f(\epsilon_z^\alpha) - f(\epsilon_z^\beta))] = \frac{n}{n_0}. \quad (65)$$

At $p_0a = 0.4$ and $T = 0$, the scaled gap parameter and the corresponding thermodynamic potential are, respectively, shown in Figs.8 and 9. The total number n is chosen as the one in the symmetric system with chemical potential μ_0 . Like the case we discussed in the last section, the BP state starts at $\delta\mu = \Delta_0/2$ with the gap parameter $\Delta < \Delta_0$, but it is always instable in the whole asymmetry region. The BCS solution is stable in weak asymmetry region $0 < \delta\mu < \Delta_0/\sqrt{2}$, and the normal liquid gas becomes stable in strong asymmetry region $\delta\mu > \Delta_0/\sqrt{2}$.

When the LOFF state is included, by combining the thermodynamic potential (60) and the gap equations (58) together with the total particle number

$$\begin{aligned} \int_0^\Lambda dz \sqrt{z} \int_{-1}^1 dx [1 + (U_z^2 - V_z^2) (f(E_{z,x}^A) - f(E_{z,x}^B))] \\ = 2 \frac{n}{n_0}, \end{aligned} \quad (66)$$

the LOFF gap is also shown in Fig.8 and the LOFF momentum is indicated in Fig.10 for the two branches

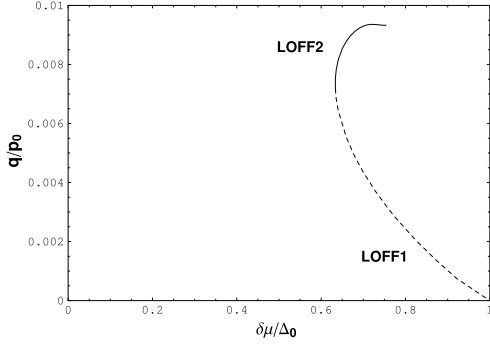


FIG. 10: The scaled LOFF momentum as a function of the scaled chemical potential difference at $p_0a = 0.4$ and $T = 0$ for LOFF1 and LOFF2.

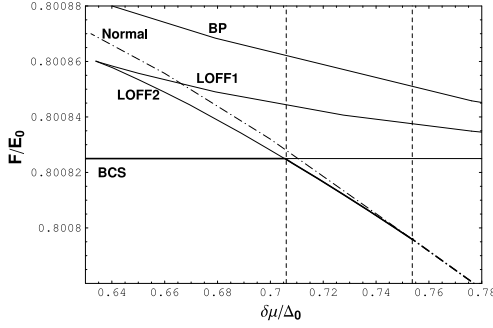


FIG. 11: The scaled free energy as a function of the scaled chemical potential difference at $p_0a = 0.4$ and $T = 0$ for normal, BCS, BP, and LOFF (LOFF1, LOFF2) states. The thick lines indicate the real ground states in different regions.

LOFF1 and LOFF2. From the comparison of the free energies for normal, BCS, BP, LOFF1, and LOFF2 states, shown in Fig.11, the LOFF2 state is the real ground state in the intermediate asymmetry region $\Delta_0/\sqrt{2} = 0.707\Delta_0 < \delta\mu < 0.754\Delta_0$. In summary, the case with fixed n and $\delta\mu$ is very similar to the case with fixed μ and $\delta\mu$, the narrow asymmetry window for the LOFF state is the same in the two cases. However, this conclusion depends on the assumption of $m_a = m_b$. For systems with large mass difference between the two species, the two cases are probably very different[66].

VIII. FIXED PARTICLE NUMBERS

We now turn to the case of fixed numbers n_a and n_b of the two species, this is the case we are especially interested in. The essential quantity to describe the thermodynamics of the system is the free energy defined as

$$F = \Omega + \mu_a n_a + \mu_b n_b. \quad (67)$$

In general case of $n_a \neq n_b$, instead of n_a and n_b , we can equivalently describe the system by the total number

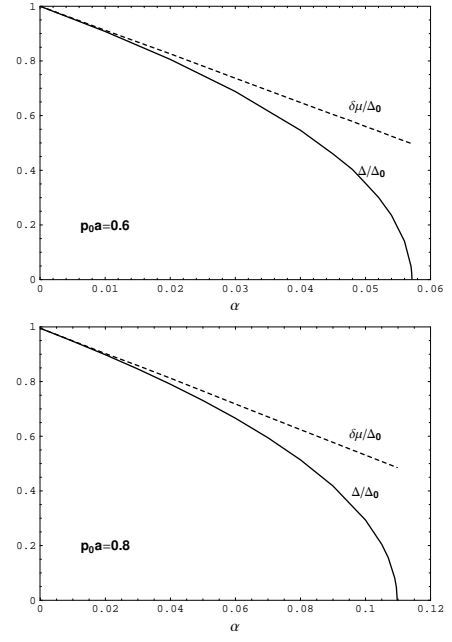


FIG. 12: The gap parameter Δ and the chemical potential difference $\delta\mu$, scaled by the symmetric gap Δ_0 , as functions of the degree of asymmetry α at $p_0a = 0.6$ and 0.8 and $T = 0$.

$n = n_a + n_b$ and the quantity

$$\alpha = \frac{n_b - n_a}{n_b + n_a}, \quad (68)$$

which controls the degree of asymmetry between the two species and satisfies $0 < \alpha < 1$. Obviously, for $n_a \neq n_b$ or $\alpha \neq 0$, the BCS pairing mechanism is ruled out, only the normal phase and BP phase are left as possible uniform ground states.

Considering the coupled set of equations for the gap parameter (57), the thermodynamic potential (59) and the particle numbers (61) with

$$\frac{n_a}{n_0} = \frac{1 - \alpha}{2} \frac{n}{n_0}, \quad \frac{n_b}{n_0} = \frac{1 + \alpha}{2} \frac{n}{n_0}, \quad (69)$$

and taking again n as its value in the symmetric system with chemical potential μ_0 , the gap parameter Δ and chemical potential difference $\delta\mu$ in the BP state as functions of α are shown in Fig.12 at $p_0a = 0.6$ and 0.8 and $T = 0$. While both Δ and $\delta\mu$ drop down with increasing degree of asymmetry, they always satisfy the condition for the BP state, $\Delta < \delta\mu$, and the difference between them becomes larger and larger. Finally, they end at a critical value $\alpha_c^{BP} = 0.057$ for $p_0a = 0.6$ and 0.11 for $p_0a = 0.8$. From the comparison with Fig.3 in the case with fixed μ and $\delta\mu$ and Fig.8 in the case with fixed n and $\delta\mu$, the BP gap parameter here still starts with $\Delta = 0$ at $\delta\mu = \Delta_0/2$ and ends with $\Delta = \Delta_0$ at $\delta\mu = \Delta_0$. The α -dependence of Δ and $\delta\mu$ and the critical value α_c^{BP} in our calculation agree well with the analytic results obtained

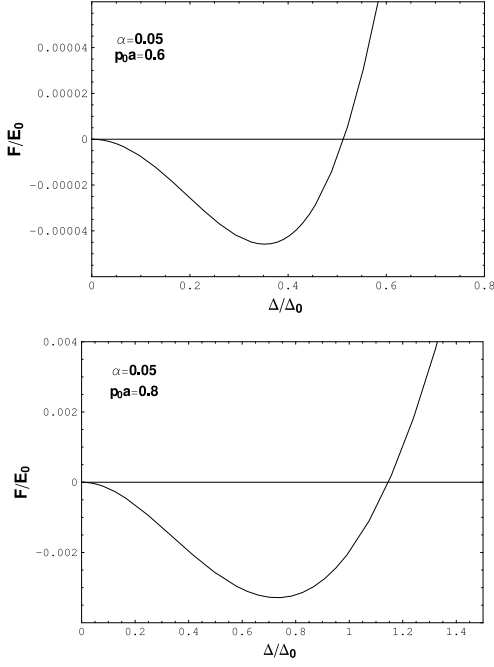


FIG. 13: The scaled free energy as a function of the scaled gap parameter at zero temperature, fixed degree of asymmetry $\alpha = 0.05$ and fixed interaction strength $p_0a = 0.6$ and 0.8 . The minimum and maximum correspond, respectively, to the BP and normal states.

in weak interaction limit[67, 68],

$$\begin{aligned} \frac{\Delta(\alpha)}{\Delta_0} &= \sqrt{1 - \frac{\alpha}{\alpha_c^{BP}}}, \\ \frac{\delta\mu(\alpha)}{\Delta_0} &= 1 - \frac{1}{2} \frac{\alpha}{\alpha_c^{BP}}, \\ \alpha_c^{BP} &= \frac{3}{4} \frac{\Delta_0}{\mu_0} = \frac{6}{e^2} e^{-\frac{\pi}{2p_0a}}. \end{aligned} \quad (70)$$

The question is which of the normal and BP states is relatively stable? From the direct calculation of the free energy as a function of the gap parameter at $\alpha = 0.05$, $p_0a = 0.6$ and 0.8 and $T = 0$, shown in Fig.13, the trivial solution $\Delta = 0$ is the maximum but the BP solution $\Delta \neq 0$ is the minimum of the free energy. Therefore, the Sarma instability is avoided and BP becomes a stable solution in the family of spatially uniform phases. It is necessary to emphasize that the point to avoid the Sarma instability is the constraint of unequal numbers of the two species.

The LOFF solution is obtained through calculating the gap equations (58) for the LOFF gap and LOFF momentum, the thermodynamic potential (60) and the number constraints (62) with n_a and n_b given by (69). At zero temperature, the LOFF gap and LOFF momentum are plotted as functions of the degree of asymmetry α in Figs.14 and 15 for $p_0a = 0.6$ and 0.8 . From the behavior of the LOFF gap parameter Δ relative to

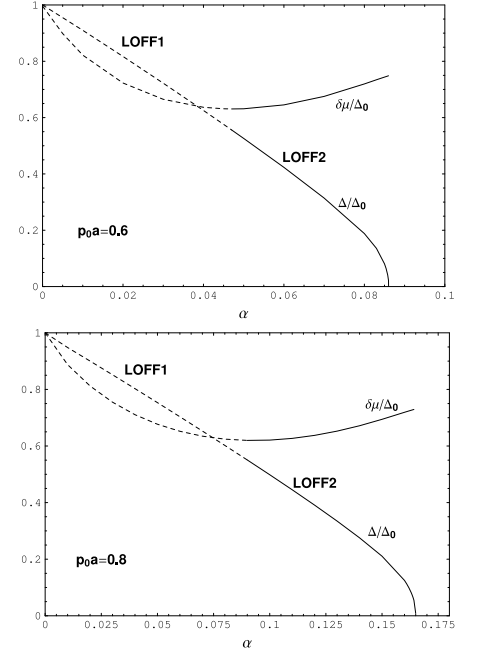


FIG. 14: The scaled LOFF gap Δ and chemical potential difference $\delta\mu$ as functions of the degree of asymmetry α at $T = 0$ and $p_0a = 0.6$ and 0.8 . The dashed and solid lines correspond, respectively, to the branches LOFF1 and LOFF2.

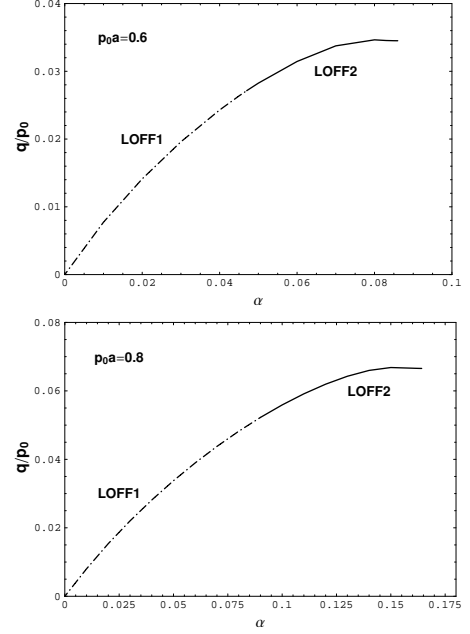


FIG. 15: The scaled LOFF momentum q as a function of the degree of asymmetry α at $T = 0$ and $p_0a = 0.6$ and 0.8 .

the chemical potential difference $\delta\mu$, we can separate the LOFF solution into two branches, LOFF1 and LOFF2. Exactly the same as what shown in Figs.3 and 8, the two branches meet at $\delta\mu = 0.635\Delta_0$, LOFF1 ends with $\Delta = \Delta_0$ at $\delta\mu = \Delta_0$, and LOFF2 ends with $\Delta = 0$ at $\delta\mu \simeq 0.754\Delta_0$. If we denote the asymmetry correspond-

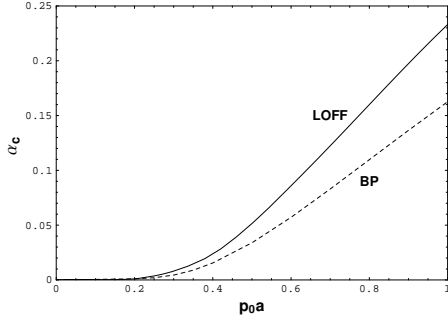


FIG. 16: The critical values of α for BP and LOFF states as functions of the interaction strength $p_0 a$.

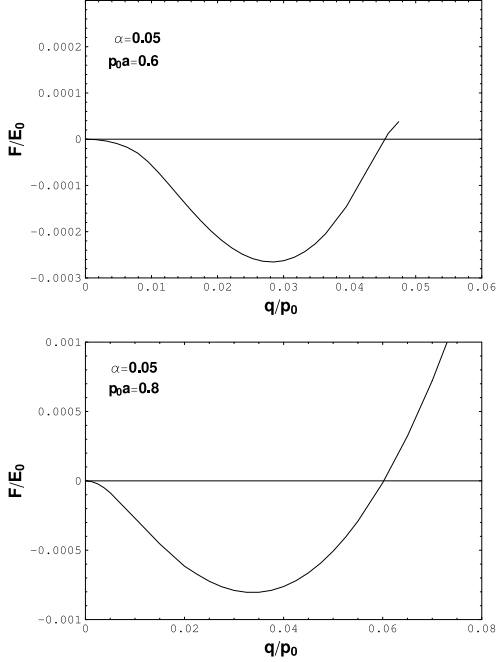


FIG. 17: The scaled free energy as a function of the pair momentum q/p_0 at fixed degree of asymmetry and two values of coupling strength. The maximum at zero pair momentum and the minimum at finite pair momentum correspond, respectively, to the BP and LOFF states.

ing to the meeting point of LOFF1 and LOFF2 as α_0 , LOFF1 is in the region $0 < \alpha < \alpha_0$ and LOFF2 in the region $\alpha_0 < \alpha < \alpha_c^{LOFF}$, where α_c^{LOFF} is the critical asymmetry for the LOFF state. From the comparison with the critical value α_c^{BP} for the BP state shown in Fig.12, we have $\alpha_c^{LOFF} > \alpha_c^{BP}$. Therefore, when the number difference between the two species is large enough, there is only LOFF superfluidity in the system. From Fig.16, the difference between the two critical values increases with increasing coupling strength. It is also necessary to note that the condition for the BP gap parameter, $\Delta < \delta\mu$, is no longer necessary for the LOFF gap parameter, because of the term pqx/m in the dispersion relation (37).

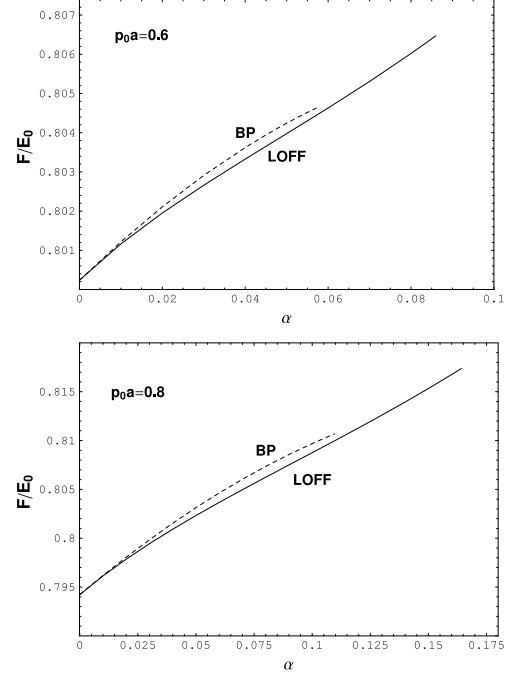


FIG. 18: The free energies for the BP and LOFF states as functions of the degree of asymmetry at two values of the coupling strength.

Now the question left is to extract the real ground state from the uniform and non-uniform phases. Since we have done the stability analysis for the two uniform states and the normal phase is already kicked out, we need to compare the free energies only for the BP and LOFF states. Fig.17 shows the free energy as a function of the pairing momentum at a fixed degree of asymmetry and two values of the coupling strength. It is clear that the BP state which has a zero pair momentum is a maximum of the free energy, while the LOFF state which has a finite pair momentum is the minimum of the free energy. From the α -dependence of the free energies for BP and LOFF states at two values of the coupling strength, shown in Fig.18, we have the conclusion that, in the coexistence region of BP and LOFF states, LOFF is the stable one, and in the region with strong asymmetry, the BP disappears, and the LOFF becomes the only possible mechanism for superfluidity. It is necessary to point out that, while only a part of LOFF2 is stable in the case with fixed μ and $\delta\mu$ or the case with fixed n and $\delta\mu$, both LOFF1 and LOFF2 are stable in the case with fixed n_a and n_b .

IX. SUMMARY

The key theoretic problem in the study of fermion superfluidity is the pairing mechanism. For the asymmetric fermion superfluidity which promotes new interests recently in both traditional fields like condensed matter physics and atom physics and newly developed color

superconductivity study in high energy physics, the familiar pairing phases include spatially uniform BCS and BP states and spatially non-uniform LOFF state. A hot topic in the investigation is which is the real ground state for a system under some physical constraints which lead to mismatched Fermi surfaces of the two species.

We have investigated the competition between the uniform normal, BCS, BP phases and non-uniform LOFF phase in asymmetric fermion superfluids in the frame of a general four fermion interaction model in weak coupling region. The masses of the two species of fermions m_a and m_b are set to be equal, but their chemical potentials μ_a and μ_b can be different under some physical conditions. Three cases which we are most interested in are discussed: (1) the chemical potentials μ_a and μ_b are directly fixed, (2) the total number and the chemical potential difference are fixed, and (3) the numbers of the two species are separately fixed.

In BP phase, there are two kinds of instabilities, one is the Sarma instability which was found many years ago, and the other is the magnetic instability which was recently pointed out in the study of gapless color superconductivity. While the magnetic instability gives us a strong hint that the LOFF phase may be stabler than the BP phase, to confirm this statement needs the comparison of the free energies for the normal, BCS, BP and LOFF states, when the chemical potentials of the two species are not directly fixed. By solving the gap equations, we firstly obtained all possible solutions, and then by comparing the thermodynamic potentials Ω or free energies F for the four phases, we determined the real ground state which corresponds to the lowest minimum of Ω or F . For case (1) and case (2), the BP state is always unstable due to the Sarma instability, the system is in BCS phase when the chemical potential difference is small and in normal phase when the difference is large enough, and the LOFF state can exist only in a narrow window of asymmetry. For case (3), the Sarma instability of the BP state can be avoided due to the disappearance of the BCS phase, if n_a and n_b are set to be unequal. However, due to the magnetic instability of the

BP state, in the coexistence region of BP and LOFF, the LOFF state is always the stable one. In addition, the LOFF state can even survive when the BP disappears in the highly asymmetric region.

The LOFF state is not yet experimentally confirmed in the study of fermion superfluidity and superconductivity. Our conclusion is that, it may be observed in asymmetric fermion systems when the numbers of the two species are fixed and different, for instance, in trapped atomic fermion system. Recently, this topic was discussed in [35, 36], and an investigation with a low dimensional integral model showed that the LOFF phase is favored in weak coupling region[40].

Some questions are still open:

1) We considered in this paper only the asymmetric systems where the masses of the two kinds of fermions are set to be equal. The system with mass difference between the two species is of great interest, since it can be realized in an atomic fermion gas with a mixture of different fermionic atoms such as ^6Li and ^{60}K [5]. As we have shown in [56], the magnetic instability may be killed when the mass ratio of the two species becomes very large. The true ground state of these systems is still unknown and needs further investigation.

2) The spatially mixed phase of the normal, BCS and BP states is not considered in this paper, and hence our conclusion is not completed. It has been shown in [9, 69] that the mixed phase is probably the ground state in the case with fixed numbers. However, the LOFF phase is not yet included in the study.

3) The superfluidity we considered here is non-relativistic, which can be applied to the study of electronic system, atomic fermion gas and nuclear matter. What is the relativistic effect? This is still not very clear but of great interest for the study of cold color superconducting quark matter. Some approximate calculations in this field are presented recently[59, 63].

Acknowledgement: The work was supported in part by the grants NSFC10428510, 10435080, 10447122, 10575058 and SRFDP20040003103.

-
- [1] G.Sarma, J.Phys.Chem.Solid **24**,1029(1963).
 - [2] A.I.Larkin and Yu.N.Ovchinnikov, Sov.Phys. JETP **20**(1965).
 - [3] P.Fulde and R.A.Ferrell, Phys. Rev **A135**,550(1964).
 - [4] S.Takada and T.Izuyama, Prog.Theor.Phys.**41**,635(1969).
 - [5] W.V.Liu and F.Wilczek, Phys. Rev. Lett.**90**, 047002(2003).
 - [6] H.H.Suhl, B.T.Matthias and L.R.Walker, Phys.Rev.Lett.**3**,552(1959).
 - [7] J.Kondo, Prog.Theor.Phys.**29**,1(1963).
 - [8] J.I.Cirac and P.Zoller, Physics Today **57**,38(2004).
 - [9] H.Caldas, Phys. Rev. **A69**, 063602(2004).
 - [10] A.Sedrakian and U.Lombardo, Phys. Rev. Lett. **84**, 602(2000).
 - [11] T.Schäfer and F.Wilczek, Phys. Rev. **D60**, 074014 (1999).
 - [12] M.Alford, J.Berbgas, and K.Rajagopal, Nucl. Phys. **B558**, 219 (1999).
 - [13] K.Rajagopal and F.Wilczek, Phys. Rev. Lett. **86**, 3492 (2001).
 - [14] A.W.Steiner, S.Reddy, and M.Prakash, Phys. Rev. **D66**, 094007(2002).
 - [15] M.Alford and K.Rajagopal, JHEP **06**, 031(2002).
 - [16] M.Huang, P.Zhuang, and W.Chao, Phys. Rev. **D67**, 065015(2003).
 - [17] I.Shovkovy and M.Huang, Phys. Lett. **B564** 205(2003).
 - [18] M.Huang and I.Shovkovy, Nucl. Phys. **A729**, 835(2003).

- [19] M.Alford, C.Kouvaris and K. Rajagopal, Phys. Rev. Lett. **92**, 222001(2004).
- [20] H.Abuki, M.Kitazawa, and T.Kunihiro, hep-ph/0412382.
- [21] S.B.Ruster, V.Werth, M.Buballa, I.A.Shovkovy and D.H.Rischke, Phys. Rev. **D72**, 034004 (2005).
- [22] D.Blaschke, S.Fredriksson, H.Grigorian, A.M.Oztas, and F.Sandin, hep-ph/0503194.
- [23] M.M.Forbes, E.Gubankova, W. Vincent Liu, F.Wilczek, Phys. Rev. Lett.**94**, 017001(2005).
- [24] J.Liao and P.Zhuang, Phys. Rev. **D68**, 114016(2003).
- [25] M.Alford, J.Bowers and K.Rajagopal, Phys.Rev. **D63**,074016 (2001).
- [26] J.Bowers, J.Kundu, K.Rajagopal and E.Shuster, Phys.Rev. **D64**,014024(2001).
- [27] A.K.Leibovich, K.Rajagopal and E.Shuster, Phys.Rev. **D64**, 094005(2001).
- [28] R.Casalbuoni, R.Gatto, M.Mannarelli and G.Nardulli, Phys.Lett. **B511**, 218(2001).
- [29] R.Casalbuoni and G.Nardulli, Rev.Mod.Phys. **76**, 263(2004).
- [30] R.Casalbuoni, M.Ciminale, M.Mannarelli, G.Nardulli, M.Ruggieri, R.Gatto, Phys.Rev. **D70**, 054004(2004).
- [31] A.Sedrakian, Phys.Rev. **C63**, 025801(2001).
- [32] H.Muether and A.Sedrakian, Phys.Rev. **C67**, 015802(2003).
- [33] A.Sedrakian, J.Mur-Petit, A.Polls and H.Mther, Phys.Rev. **A72**, 013613(2005).
- [34] P.Castorina, M.Grasso, M.Oertel, M.Urban, D.Zappala, Phys.Rev. **A72**, Phys.Rev. A72 025601(2005).
- [35] T.Mizhushima, K.Machida and M.Ichioka, Phys.Rev.Lett.**94**, 060404(2005).
- [36] Kun Yang, Phys.Rev.Lett.**95**, 218903(2005).
- [37] D.T.Son and M.A.Stephanov, cond-mat/0507586.
- [38] D.E.Sheehy and L.Radzihovsky,cond-mat/0508430.
- [39] Kun Yang, cond-mat/0508484.
- [40] J.Dukelsky, G.Ortiz and S.M.A. Rombouts, cond-mat/0510635.
- [41] M.Huang and I.Shovkovy, Phys.Rev. **D70**, R051501(2004).
- [42] M.Huang and I.Shovkovy, Phys. Rev. **D70**, 094030(2004).
- [43] R.Casalbuoni, R.Gatto, M.Mannarelli, G.Nardulli and M.Ruggieri, Phys.Lett. **B605** 362(2005).
- [44] M.Alford, Q.Wang, J.Phys. **G31** 719(2005).
- [45] K.Fukushima, hep-ph/0506080.
- [46] P.Svedlindh, K.Niskanen, P.Norling, et al., Physica C **162-164**,1365(1989).
- [47] W.Braunisch, N.Knauf, V.Kataev, et al., Phys. Rev. Lett. **68**,1908(1992); W.Braunisch, N.Knauf, G.Bauer, et. al., Phys.Rev.B.**48**,4030(1993).
- [48] D.J.Thompson, M.S.M.Minhaj, L.E.Wenger and J.T.Chen, Phys.Rev.Lett.**75**,529(1995).
- [49] P.Kosti, B.Veal, A.P.Paulikas, et al., Phys.Rev.B.**53**,791(1996); Phys.Rev.B.**55**,14649(1997).
- [50] F.M.Araujo-Moreira, P.Barbara, A.B.Cawthorne and C.J.Lobb, Phys.Rev.Lett.**78**,4625(1997).
- [51] P.Barbara, F.M.Araujo-Moreira, A.B.Cawthorne and C.J.Lobb, Phys.Rev.B.**60**,7489(1999).
- [52] M.Sigrist and T.M.Rice, Phys.Soc.Jpn.**61**,4283(1992).
- [53] K.M.Lang, Nature(London) **415**,412(2002).
- [54] M.Sigrist and T.M.Rice, Rev.Mod.Phys. **67**, 503(1995).
- [55] M.S.Li, Phys. Reports **376**, 133(2003).
- [56] L.He, M.Jin and P.Zhuang, hep-ph/0509317, Phys.Rev. **B** accepted.
- [57] I.Giannakis and H.Ren, Phys. Lett. **B611**, 137(2005).
- [58] I.Giannakis and H.Ren, Nucl. Phys. **B723**, 255(2005).
- [59] I.Giannakis, D.Hou and H.Ren, Phys.Lett. **B631** 16(2005).
- [60] M.Huang, hep-ph/0504235.
- [61] D.Hong, hep-ph/0506097.
- [62] E.V.Gorbar, M.Hashimoto and V.A.Miransky, hep-ph/0507303.
- [63] E.V.Gorbar, M.Hashimoto and V.A.Miransky, hep-ph/0509334.
- [64] R.Casalbuoni, R.Gatto, N.Ippolito, G.Nardulli and M.Ruggieri, Phys.Lett. **B627** 89(2005).
- [65] T.Papenbrock and G.F.Bertsch, Phys. Rev. **C59**, 2052(1999).
- [66] E.Gubankova, W.V.Liu, F.Wilczek, Phys. Rev. Lett. **91**, 032001 (2003).
- [67] J.Mur-Petit, A.Polls and H.-J.Schulze, Phys.Lett.A **290**, 317(2001)
- [68] U.Lombardo, P.Nozieres, P.Schuck, H.-J.Schulze and A.Sedrakian, Phys.Rev.C **67**, 015802(2003)
- [69] P.F.Bedaque, H.Caldas and G.Rupak, Phys. Rev. Lett. **91**, 247002(2003).